Tetrahedron 69 (2013) 9045–9055

Contents lists available at ScienceDirect

Tetrahedron

journal homepage: www.elsevier.com/locate/tet

Unsymmetric 1,3,4-oxa(thia)diazoles of quinoxaline–naphthalene conjugates

Kuan-Ting Lin [a], Hsiu-Ming Kuo [a], Hwo-Shuenn Sheu [b], Chung K. Lai [a,*]

[a] Department of Chemistry, National Central University, Chung-Li 32001, Taiwan, ROC
[b] National Synchrotron Radiation Research Center, Hsinchu 30077, Taiwan, ROC

ARTICLE INFO

Article history:
Received 27 May 2013
Received in revised form 24 July 2013
Accepted 15 August 2013
Available online 22 August 2013

Keywords:
1,3,4-Oxadiazoles
1,3,4-Thiadiazoles
Quinoxalines
Naphthalenes
Hexagonal columnar phases
Liquid crystals

ABSTRACT

Two new series of unsymmetric 1,3,4-oxa(thia)diazoles **1a**,**b** containing both quinoxaline and naphthalene moieties were prepared and their mesomorphic properties were investigated. The mesomorphic behavior of compounds **1a**,**b** and **2** was studied by DSC analysis and polarized optical microscopy. All compounds **1a** and **2** exhibited hexagonal columnar phases (Col_h), which were also confirmed by powder XRD diffractometer. N_{cell} and R_{ar} values equal to 5.23 and 22.73 Å^2 within a slice of 9.0 Å thick were also obtained for **1a** (n=16), indicating that a more disc-like structure constructed by two molecules lying side-by-side was correlated in Col_h phases. In contrast, all compounds **1b** were not mesogenic, and the lack of mesomorphic properties in **1b** might be due to their unfavorable conformations. The PL spectra of all compounds **1a**,**b** showed one intense peak at λ_{max}=509–512 nm, and these photoluminescent emissions originated from quinoxaline moiety.

1. Introduction

1,3,4-Oxadiazole (OXD), considered as one of a few important compounds among five-membered ring heterocycles has been paid more attention in the field of materials chemistry due to their excellent thermal and chemical stabilities. 1,3,4-Oxadiazoles are structurally interesting; they are bent-shaped structures, electron-deficient rings, and good electron-acceptors. They were excellent candidates as blue emitters, and have applications[1] in OLED devices. Numerous known 1,3,4-oxadiazoles with a variety of novel structures were studied as electron transporting materials in OLED and widely applied as organic electron conductors. The first mesogenic asymmetric 1,3,4-oxadiazole was reported[2] by Dimitrowa et al. Thereafter more examples of mesogenic 1,3,4-oxadiazoles[3] with either symmetrical or asymmetrical structures were prepared and studied. Furthermore, a few mesogenic bi(1,3,4-oxadiazoles)[4] or tri(1,3,4-oxadiazoles)[5] were also reported. Nematic or layer smectic phases formed by these linear-shaped or bent-shaped molecules were commonly observed. In contrast, lesser examples exhibiting columnar phases[5b,6] were also known. 1,3,4-Oxadiazole is structurally nonlinear and has a larger exocyclic bond angle[7] ($\varepsilon \sim 135°$), which often resulted in a dramatic lowering both in melting or/and clearing points. This was an important key factor in processing commercial display technology. Hydrogen-bonded mesogenic oxadiazoles[8] mixed with pyridines or acids were reported. A few examples[9a] 1,3,4-oxadiazoles **I** and their metallomesogens **II**[3p,9b] were previously reported by this group. In contrast, their homologue 1,3,4-thiadiazoles showed an apparently different mesomorphic behavior. The replacement of oxygen atom by sulfur atom often led to an improved mesomorphic behavior.[9a] The reason might be twofold; (1) the larger sulfur atom incorporated in heterocyclic rings was more easily polarized and better induced in the mesophases. (2) The longer C–S bond distance[10] and larger C–S–C angle facilitated its formation of a more rod-like or better linear conformation, compared to the bent-shaped 1,3,4-oxadiazoles.

Quinoxalines were also called benzopyrazines. They were highly π-conjugated backbones and were potentially useful in many applications such as dyes, organic light-emitting diodes, electroluminescence, organic thin film transistors (TFT), and organic photovoltaics when incorporated with an electron-donor and electron-acceptor units via π-bridge(s). They were also considered as half-disc, elliptical or round molecules, which could easily or spontaneously self-assemble into columns when π–π interaction or dipole–dipole interactions are accessible between neighboring molecules. These molecules capable of forming columnar stacking arrangements might have a dramatic impact propensity. A few promising materials, such as liquid crystals, light-emitting diodes,

* Corresponding author. Tel.: +886 (0)3 4259207; fax: +886 (0)3 4277972; e-mail address: cklai@cc.ncu.edu.tw (C.K. Lai).

0040-4020/$ – see front matter © 2013 Elsevier Ltd. All rights reserved.
http://dx.doi.org/10.1016/j.tet.2013.08.031

and photovoltaic devices have been explored and studied. Some known examples[11] derived from mesogenic quinoxalines **III**–**V**[12] were studied and were investigated. Compounds **III** derived from dibenzo[*a*,*c*]phenazine exhibited an improved mesomorphic behavior than compounds **IV** due to their better coplanarity. Some quinoxalines had a higher charge carrier mobility due to their highly conjugated structures. Substitutions and/or substituents positions incorporated were found to play an important role on the formation of mesophases.

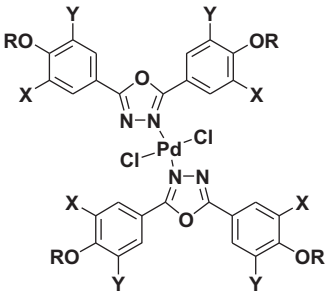

I; Cr (X = H)
Col (Y = OR)

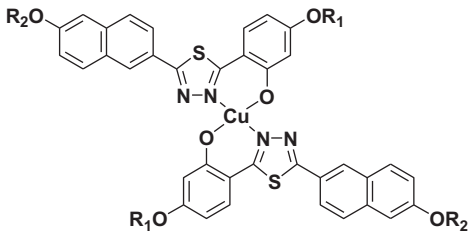

II; SmA/SmC

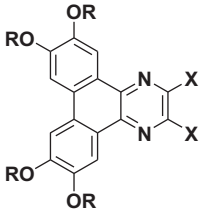

III: Cr (X = H),
Col (X = CN, OR)

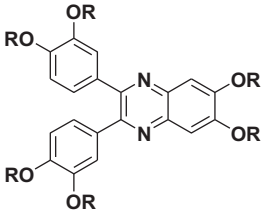

IV: Cr

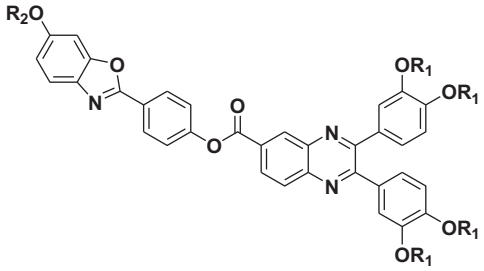

V; Col

In this work, we report the preparation and mesomorphic studies of two new series of unsymmetrical 1,3,4-oxa(thia)diazole **1a**,**b**. These were constructed by incorporating a lateral quinoxaline and naphthalene groups. Both lateral moieties were incorporated to enhance the molecular polarization and/or dipole needed to induce the mesophases. Also, π–π interactions might be also enhanced. All compounds **1a** and **2** exhibited hexagonal columnar phases (Col_h), which were also confirmed by powder XRD diffractometer. In contrast, all compounds **1b** were not mesogenic, and the lack of mesomorphic properties in **1b** might be due to their unfavorable conformation. The PL spectra of all compounds **1a**,**b** were examined.

2. Results and discussion

2.1. Synthesis and characterization

Two common synthetic routes were applied to prepare 1,3,4-oxadiazole derivatives. In this work the synthetic procedures of 1,3,4-oxa(thia)diazoles **1a**,**b** were given in Scheme 1. 1,2-Bis(3,4-didodecyloxy)phenyl)-1,2-ethanedione was obtained by the reaction of 1,2-bis (dodecyloxy)benzene with oxalyl chloride in the presence of $AlCl_3$ stirring in carbon disulfide at ice bath temperature, which was then condensed with 3,4-diaminobenzoic acid stirring in THF to give 2,3-bis-(3,4-bis(dodecyloxy)phenyl)quinoxaline-6-carboxylic acid **3**. On ^{1}H NMR spectrum, a characteristic broad peak often appeared at $\delta \sim 13.50$ ppm assigned for −COO*H* was not observed for acids **3** due to rapid exchange. However, a characteristic peak at ca. δ 170.92 ppm assigned for −*C*OOH was observed on its ^{13}C NMR spectrum. Then, 2,3-bis(3,4-bis(dodecyloxy) phenyl)-*N*′-(6-(alkoxy)-2-naphthoyl)quinoxaline-6-carbohydrazides **2** isolated as yellow-green solids were then obtained by condensation reactions of 6-(alkoxy)-2-naphthohydrazides and 2,3-bis-(3,4-bis(dodecyloxy)phenyl)quinoxaline-6-carboxylic acid **3** in stirring THF at room temperature. The reaction of 2,3-bis(3,4-bis(dodecyloxy)phenyl)-*N*′-(6-(alkoxy)-2-naphthoyl)-quinoxaline-6-carbohydrazides in refluxing phosphoryl chloride gave the 1,3,4-oxadiazoles **1a**. The products isolated as bright yellow solids were obtained after recrystallization from THF/methanol with a yield of 53–65%. In contrast, their analogue 1,3,4-thiadiazoles **1b** were prepared by the solutions of 2,3-bis(3, 4-bis(dodecyloxy)phenyl)-*N*′-(6-(alkoxy)-2-naphthoyl)-quinoxaline-6-carbohydrazides and phosphorous pentasulfide in refluxing pyridine for 24 h. The products isolated as yellow-green solids were obtained after recrystallization from THF/methanol. All final compounds **1a**,**b** and **2** were characterized by ^{1}H NMR, ^{13}C NMR, mass and elemental analysis. For instance, two characteristic broad singlet peaks occurred at δ 9.99–10.22 ppm and 10.26–10.48 ppm, assigned for amide-H (−CON*H*) of compounds **2** were appeared for the formation on the ^{1}H NMR spectra. On ^{13}C NMR spectra, observation of two peaks appeared, for example, at 163.84 and 165.52 ppm, and at 166.64 and 169.30 ppm was indicative of the formation of compounds **1a** (n=10) and **1b** (n=10), respectively. All data on mass and elemental analysis were well consistent with their structures and purities.

2.2. Phase transitions, mesomorphic behavior, and thermal stability

The mesomorphic behavior of compounds **1** and **2** was studied and characterized by differential scanning calorimetry (DSC) and polarizing optical microscopy (POM). The phase transitions and thermodynamic data for compounds **1** and **2** are summarized in Table 1. All compounds **2** (n=8, 10, 12, 14, 16) exhibited enantiotropic columnar phases based on observation under polarized microscope. Under POM, a typically pseudo focal-conic or more leaf-

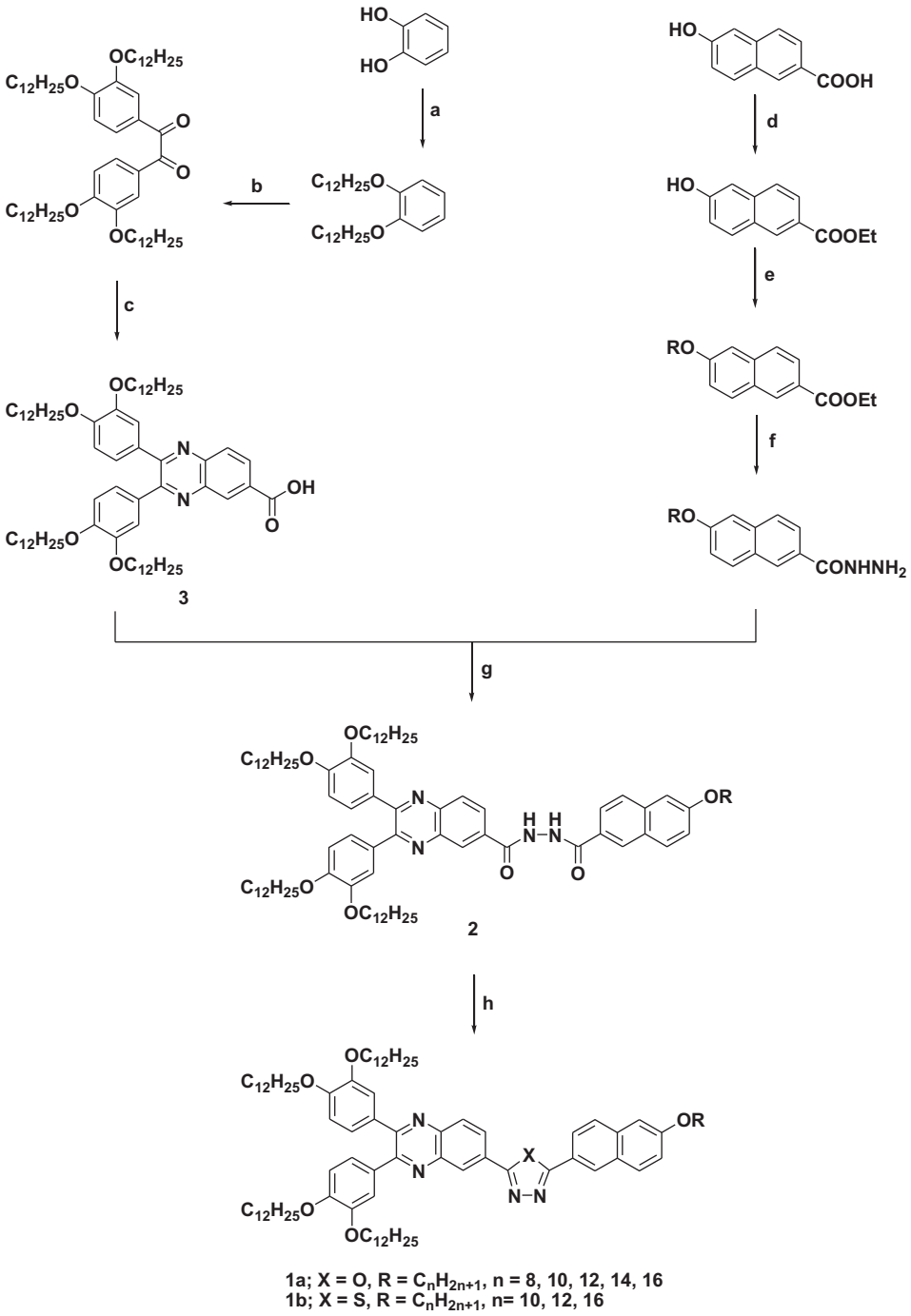

Scheme 1. Reagents and conditions: (a) RBr, K_2CO_3, and KI, refluxing in dry acetone for 48 h, 91–95%; (b) $AlCl_3$, oxalyl chloride, stirring in CS_2 at 0 °C for 6 h, 40–42%; (c) 3,4-diaminobenzoic acid, acetic acid, refluxing in THF for 24 h, 90–93 %; (d) ethanol, sulfuric acid, refluxing for 2 h, 72–75%; (e) RBr, K_2CO_3, and KI, refluxing in dry acetone for 24 h, 92–94%; (f) hydrazine monohydrate, refluxing in ethanol for 12 h, 94–97%; (g) $SOCl_2$, refluxing for 2 h; then, triethylamine, stirring in dry THF at rt for 24 h, 71–73%; (h) X=O, refluxing in $POCl_3$ for 24 h, 43–52 %; X=S, P_2S_5, refluxing in pyridine for 24 h, 25–30%.

like texture (see Fig. 1) with linear birefringent defects was clearly observed when cooling from their isotropic liquids. These observed textures also accompanied by a large area of homeotropic domain were characteristic for hexagonal columnar phases. The transition temperatures of column-to-crystal for all compounds **2** were not detectable on DSC thermographs, and they were all obtained by POM. The melting and the isotropic temperatures were ranged from T_{mp}=130.2 to 137.0 °C and T_{cl}=148.4 to 156.5 °C on heating process. On the other hand, the temperature ranges of columnar phases were ranged from ΔT_{col}=33.3 (n=16) to 41.9 °C (n=10). As indicated in Table 1, all compounds **1a** (n=8, 10, 12, 14, 16) exhibited monotropic columnar phases (Col), indicating that the columnar phases were kinetically unstable. One transition of crystal-to-isotropic on heating process and two transitions of isotropic-to-columnar and columnar-to-crystal ($Cr \rightarrow Col_h \rightarrow I$) on the cooling process appeared on DSC thermographs. A few more transitions of crystal-to-crystal ($Cr_1 \rightarrow Cr_2$) were also observed. The melting or clearing temperatures were much lower than those of compounds **2**. They were ranged from T_{cl}=79.3 (n=16) to 91.6 °C (n=10), and the temperature ranges of columnar phases were lower with carbon

Table 1
The phase transitions and enthalpies[a] of compounds **1** and **2**

2; n = 8	Cr_1	109.7 (72.7) / 108.0[b]	Cr_2	133.5 (77.9)	Col	148.4 (4.20) / 146.8 (4.06)	I
10	Cr_1	118.3 (22.2) / 110.0[b]	Cr_2	130.2 (22.9)	Col	153.6 (4.20) / 151.9 (4.21)	I
12			Cr	135.1 (3.29) / 112.0[b]	Col	156.5 (2.75) / 151.6 (3.00)	I
14			Cr	132.8 (0.84) / 115.0[b]	Col	155.6 (4.06) / 154.1 (4.09)	I
16			Cr	137.0[b] / 117.0[b]	Col	152.8 (4.49) / 150.3 (4.48)	I
1a; n = 8			Cr	90.0 (58.8) / 56.6 (53.5)	Col	73.9 (5.40)	I
10	Cr_1	58.2 (58.8)	Col	88.7 (30.3) / 72.1 (4.64)	Cr_2	91.6 (29.0)	I
12	Cr_1	58.2 (49.3)	Col	85.6 (42.0) / 70.7 (3.26)	Cr_2	89.4 (18.7)	I
14	Cr_1	61.9 (17.1)	Col	79.8 (1.55) / 67.0 (1.64)	Cr_2	83.9 (23.2)	I
16	Cr_1	46.0 (4.53) / 39.2 (2.89)	Cr_2	59.8 (28.2)	Col	79.3 (32.2) / 62.7 (1.28)	I
1b; n = 10					Cr	136.0 (37.6) / 126.7 (35.5)	I
12					Cr	135.2 (41.9) / 125.7 (39.6)	I
16					Cr	128.9 (34.0) / 122.6 (32.3)	I

[b]Determined by polarized optical microscope.
[a] n=the carbon numbers of terminal alkoxy chains; Cr_1, Cr_2=crystal; Col=columnar; I=isotropic phases.

lengths; ΔT_{col}=17.3 (n=8)>13.9 (n=10)>12.5 (n=12)>5.1 (n=14)>2.9 °C (n=16). A pseudo focal-conic texture (see Fig. 1) with linear birefringent defects when slowly cooled from their isotropic liquids was observed. The mesophase was also identified by powder XRD experiments as hexagonal columnar phase. The monotropic behavior and a shorter range of columnar mesophase might be attributed to their kinetically unstable conformations in the mesophases. A non-planar conformation resulted from two non-coplanar terminal phenyl groups on the quinoxaline moiety caused the molecule slightly twisted and increased its overall thickness (ca. 3.35 Å). The slightly increased thickness apparently weakened the molecular interactions within the column; therefore, a lower clearing temperature was obtained. Surprisingly, all 1,3,4-thiadiazoles **1b** were not mesogenic. One transition of crystal-to-isotropic was obtained at T_{cl}=128.9 (n=16)>135.2 (n=12)>136.0 °C (n=10). In general, most of known 1,3,4-thiadiazoles with a sulfur atom incorporated exhibited improved mesomorphic behavior than their analogue 1,3,4-oxadiazoles. This was often attributed to its better linearity and/or larger dipole, resulted from a more polarized sulfur atom than oxygen atom incorporated. The lack of mesomorphic properties induced in **1b** might be due to their unfavorable conformations. A detailed crystallographic determination should be informative in understanding their molecular packing. Unfortunately, an attempt to obtain a good single crystal was not successful.

The formation of columnar phases was often crucial to the side chain density, i.e., the larger size or the more rigid is the core group, and more side chain density is necessarily required. The central 1,3,4-oxadiazole size was relatively smaller when compared to the terminal quinoxaline moiety, leading to give an overall molecular shape of compounds **1** and **2** as an elongated triangular shape. On the other hand, two molecules arranged side-by-side were correlated to give a more disc molecule. The relationship plot between the melting temperatures, clearing temperatures, and the temperature ranges for compounds **1a**,**b** and **2** were given in Fig. 2. The thermal stability of compounds **1a**,**b** (n=10), and **2**,**3** (n=10) was also performed by thermogravimetric analyses (TGA) under nitrogen atmosphere, shown in Fig. 3. All four compounds showed good thermal stability at temperature below ca. 370 °C, with a relative thermal stability of **1a**>**1b**>**3**>**2** (all n=10). The decomposition temperatures for a 5% weight loss were listed in Table 2.

2.3. Variable-temperature powder X-ray diffractions and packing study in columnar phase

Variable-temperature powder XRD diffraction experiments were conducted to confirm the structure of the mesophases of compounds **1a** (n=16). A typical diffraction pattern of a two-dimensional hexagonal lattice with one very strong diffraction peak at lower angle and four much weaker diffraction peaks was obtained at 69.0 °C under cooling process, shown in Fig. 4. A diffraction pattern with a d-spacing at 35.48, 20.90, 18.16 Å, 13.75 and 12.26 Å, and a broad diffuse peak (4.43 Å) at wide-angle region was obtained (Table 3). This diffraction pattern corresponded to a hexagonal columnar arrangement with a d-spacing ratio of 1, $(1/3)^{1/2}$, $(1/4)^{1/2}$, $(1/7)^{1/2}$, and $(1/9)^{1/2}$ corresponding to Miller indices; 100,

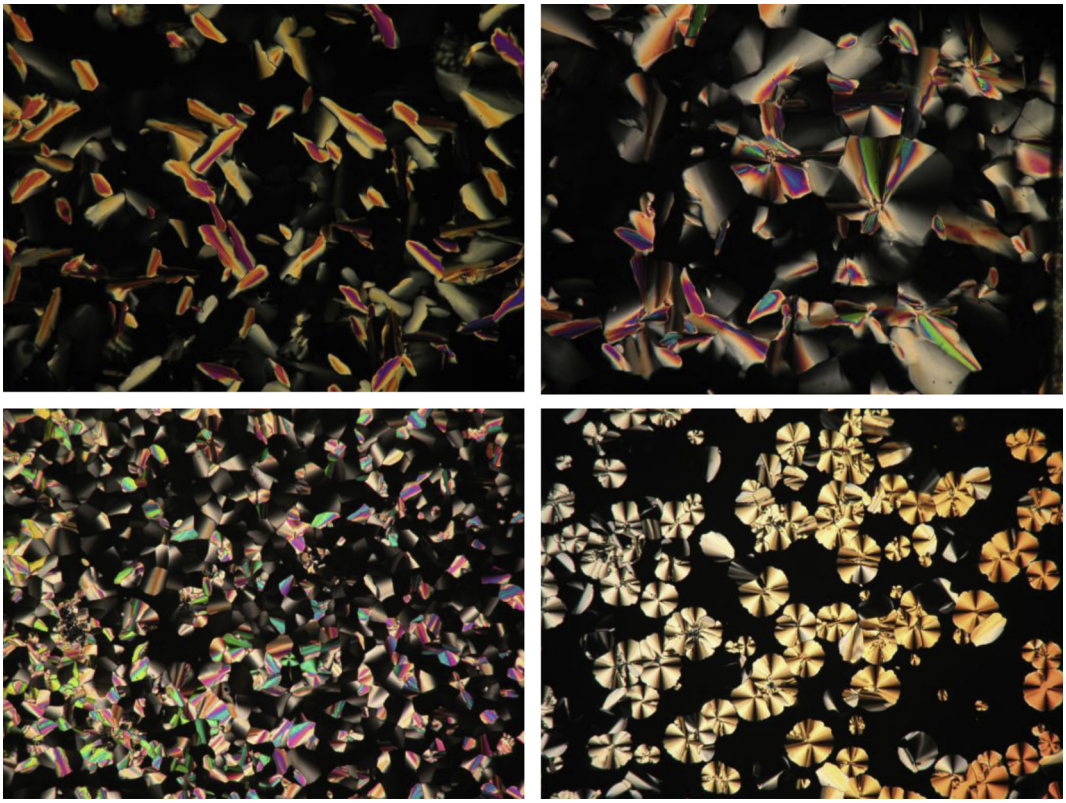

Fig. 1. Optical textures of columnar phases observed by: **2** (n=10) at 149 °C (top left) and **2** (n=14) at 153 °C (top right), **1a** (n=8) at 71 °C (bottom left) and **1a** (n=12) at 69 °C (bottom right).

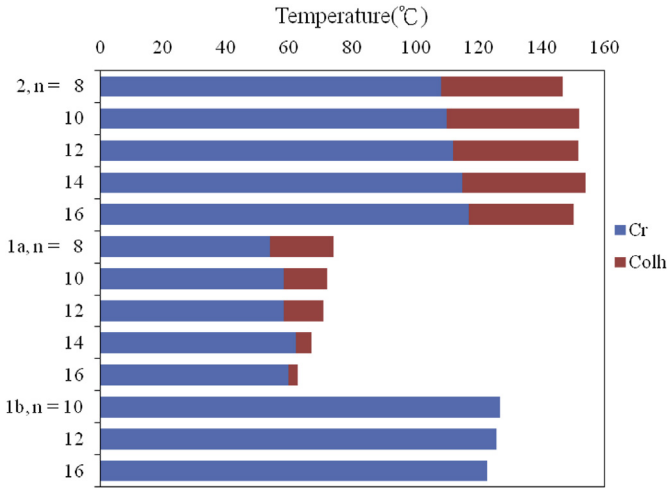

Fig. 2. Bar graphs showing the phase behavior of compounds **1a**,**b** and **2**. All temperatures were taken on the cooling process.

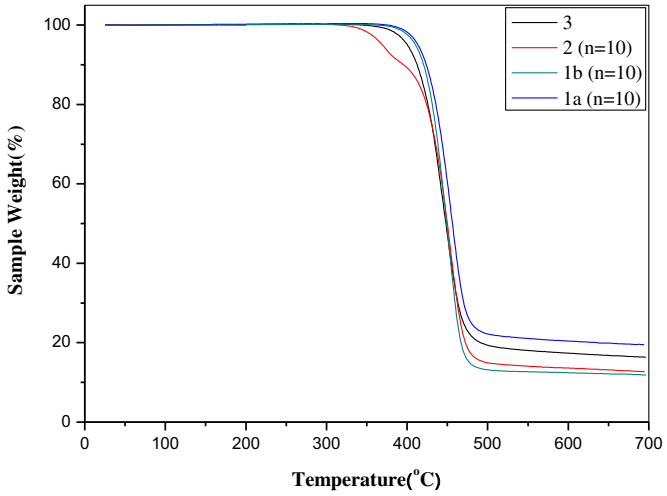

Fig. 3. The TGA thermographs of compounds **1a**,**b**, **2**, and **3** (all n=10) under nitrogen gas at a heating rate of 10.0 °C min^{-1}.

110, 200, 210, and 300, respectively. This diffraction pattern corresponds to an intercolumnar distance or lattice constant (i.e., a parameter of the hexagonal lattice) of 40.97 Å. In a hexagonal arrangement, the columns were located at the nodes of the hexagonal cell, and the columnar axes were perpendicular to the lattice plane. The lack of any relative peaks at wide angles excluded a more regular periodicity along the columns. However, liquid-like correlations between the rigid cores occurred at wide-angle regions of 4.43 Å.

In order to understand the possible molecular packing[13] in the columnar phases, the number of molecules within a portion of columnar height h was calculated by a simple model. Two important parameters, N_{cell} and R_{ar} were obtained by using XRD

Table 2
The decomposition temperatures[a] of compounds **1**–**3** by TGA analysis

Compd	T_{dec} (°C)
1a (n=10)	413.5
1b (n=10)	410.4
2 (n=10)	369.3
3	400.3

[a] Temperatures taken with a 5% weight loss.

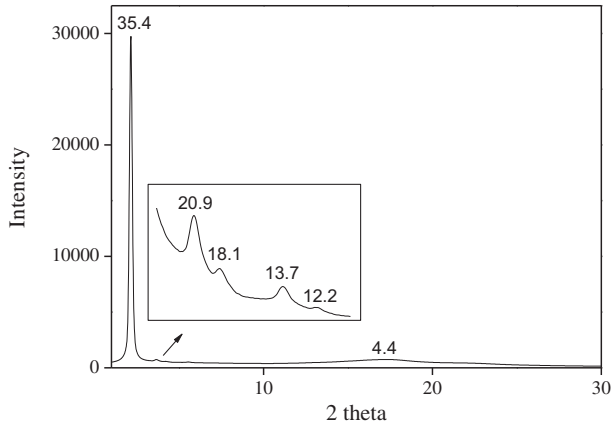

Fig. 4. The powder X-ray diffraction plot of compound **1a** (n=16) measured at 69.0 °C during the cooling process.

Table 3
Detailed indexation by powder XRD of columnar phase[a] for compounds **1a**

Compd	Mesophases temp	d-Spacing obsd (calcd)	Lattice const. (Å)	Miller indices
1a (n=16)	Col at 69.0 °C	35.48 (35.48)	a=40.97	100
		20.90 (20.48)		110
		18.16 (17.74)		200
		13.75 (13.41)		210
		12.26 (11.83)		300
		4.43 (br)		Halo

[a] Temperatures taken on the cooling process.

diffraction data. A columnar structure is often considered to be constructed by columnar cross section (S_{col}) and the stacking periodicity along the columns (h, portion of height), according to $V_{cell}=hS_{col}=N_{cell}V_{mol}$. V_{cell} is the volume of the repeat unit (per cell), and V_{mol} is the molecular volume of one molecule. N_{cell} is the number of molecules within a column. S_{col} can be calculated from lattice parameters of X-ray diffraction (Table 4).

Table 4
Geometric parameters[a] of compound **1a** (n=16)

Compd	S (Å^2)	V_{cell} (Å^3)	V_m (Å^3)	Temp (°C)	N_{cell}	S_{ar} (Å^2)	R_{ar} (Å^2)
1a (n=16)	1453.57	13,082.15	2499.92	69.0	5.23	406.04	22.73

[a] S (Å^2)=columnar cross section area, V_{cell} (Å^3)=volume of the column stratum 9 Å thick, V_m(Å^3)=molecular volume, N_{cell}=the number of molecules contained in each columnar stratum 9-Å thick, S_{ar} (Å^2)=the surface area of hard columnar core, R_{ar} (Å^2)=the diameter of the aromatic part.

On the other hand, V_{mol} is equal to the rigid part V_{ar} and the flexible chains V_{ch} by the equation. Another parameter R_{ar} is defined as the diameter of the aromatic or hard columnar part, which can be calculated by $R_{ar}=(4S_{ar}/\pi)^{1/2}$. By this simple approach, the N_{cell} and R_{ar} parameters for compounds **1a** (n=16) were then calculated. A value of N_{cell}=5.23 and R_{ar}=22.73 Å^2 at 69 °C was obtained. The R_{ar} value was close to 19.25 Å, which is the size of central core of **1a**. On the other hand, an average number of ca. 5.23 molecules for **1a** were stacked within a height of 9.0 Å in the columnar phases. Two terminal phenyl groups of quinoxaline were in fact not coplanar, leading to give a thicker molecule. A thickness of two phenyl groups twisted by an angle of approximately ca. 3.35 Å was obtained from our similar quinoxaline system.[12] The molecular shapes of compounds **1a** were not perfectly round molecules. Therefore, a more disc-like correlated structure constructed by two molecules lying roughly side-by-side was then generated within the column. The possible molecular arrangement in columnar phases was proposed in Fig. 5. The proposed packing style was quite consistent with our previous studies of quinoxaline–benzoxazole conjugates. Two molecules lying above and below plane were arranged in an antiparallel head-to-tail into a layer structure, and also π–π interactions as point to face were observed.

2.4. Optical properties

The UV–vis absorption and PL spectra of the compounds **1**–**3** (all n=10) measured in CH_2Cl_2 solution at room temperature are presented in Fig. 6. The λ_{max} peaks of UV–vis absorption and PL spectra were listed in Table 5. The absorption λ_{max} peaks of compounds **1a**,**b** occurred at ca. 280–287 and 402–405 nm, which were attributed to n–π* and π–π* transitions arising from quinoxaline moiety.[12] The 1,3,4-thiadiazole **1b** has its inherent absorption peak slightly red shifted by 28 nm over 1,3,4-oxadiazole **1a**. The other peak occurred at 324–352 nm was assigned to n–π*. The peak occurred at ca. 306 nm was assigned to amide group. The PL spectra of all compounds **1a**,**b** showed one intense and broad peak occurred at λ_{max}=509–517 nm, and this photoluminescent emission originated from heterocyclic quinoxaline.[12] In general, the electronic natures of substitution groups; for example, incorporated donors or acceptors often shifted the emission peaks. An apparent red-shift was often observed when an electron-donating group was incorporated. However, the photoluminescent emission peaks by 1,3,4-oxadiazoles often appeared at ca. 390–418 nm[4a,g,9a,b,14c] were not observed in this system and incorporation of a highly extended-conjugated quinoxaline would not shift its λ_{max}. Both quinoxaline and 1,3,4-oxa(thia)diazoles were often considered as π-acceptors and fluorophore. A red-shift emission often attributed to donor–acceptor transfer was also not observed. The lack of an emission by 1,3,4,-oxadiazoles[3] at ca. 390–418 nm was probably attributed to the so-called fluorescence resonance energy transfer (FRET).[14] Fluorescence resonance energy transfer, also known as Förster resonance energy transfer, is a non-radiative process in which the resonance energy transfers from an excited state of a donor fluorophore (D–F) to the ground state of an acceptor fluorophore (A–F) via a non-radiative 'dipole–dipole coupling'. The emission peaks of D–F were expected to have some overlap with the absorption peaks of A–F. On the other hand, the energy emitted by 1,3,4-oxadiazole at ca. 400 nm was absorbed by quinoxaline, and then emitted an emission at 509–512 nm, as shown in Fig. 7. The PL spectra of **1a**,**b** were also obtained by using 324 nm (for **1a**-10) and 352 nm (**1b**-10) as their excitation wavelengths, and the two values of λ_{max}=508 and 505 nm were obtained for **1a** (n=10) and **1b** (n=10). A slightly higher quantum efficiency ranged from 0.55 to 0.57% was obtained due to the FRET effect.

3. Conclusions

Two new series of heterocyclic 1,3,4-oxa(thia)diazoles **1a**,**b** constructed by quinoxaline–naphthalene conjugates incorporated as terminal moieties were prepared and their mesomorphic properties were investigated. All precursors **2** and **1a** formed hexagonal columnar phases, in contrast, all compounds **1b** were non-mesogenic. N_{cell} and R_{ar} values equal to 5.23 and 22.73 Å^2 within a slice of 9.0 Å thick were obtained for **1a** (n=16), indicating that a more disc-like correlated structure constructed by two molecules lying side-by-side was packed in Col_h phases. The PL spectra of all compounds **1a**,**b** showed one intense peak occurred at ca. λ_{max}=509–512 nm, which originated from quinoxaline moiety. The lack of an emission by 1,3,4-oxadiazoles at ca. 390–418 nm was probably attributed to the FRET process.

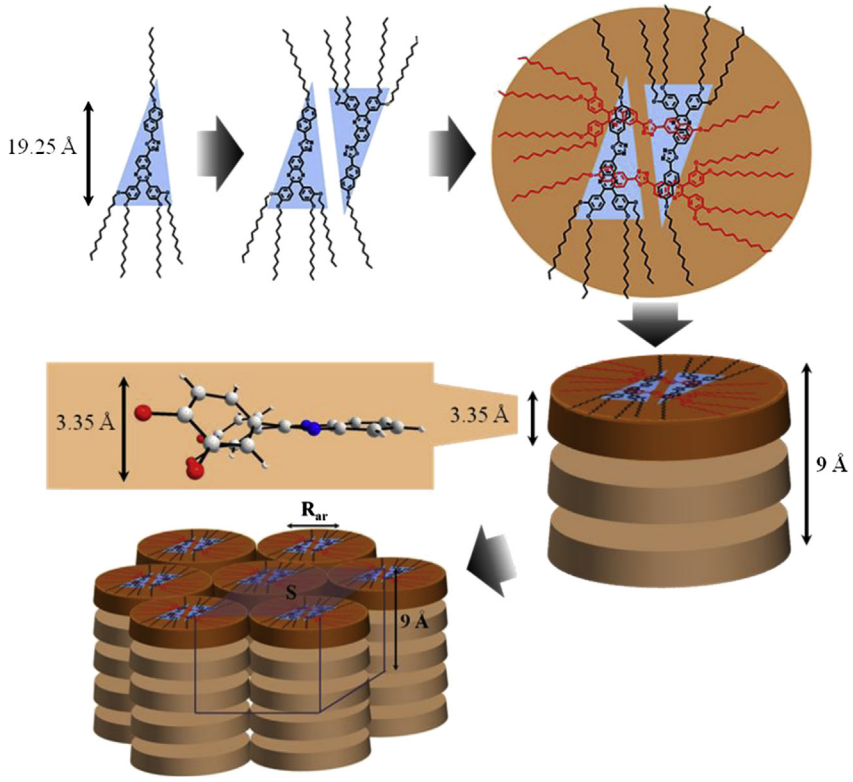

Fig. 5. A schematic representation of molecular organization in columnar phase by compounds **1a** (n=16). Two tapered-shaped molecules lying side-by-side to generate a more disc-correlated molecule was packed within a column. In a typical calculation a value of 9.0 Å ($2h$=9.0 Å) has been assumed for most discotic molecules corresponding to the board signal observed in the XRD diffraction patterns. A thickness of ca. 3.35 Å was obtained from crystallographic data of a similar quinoxaline reported.[12]

4. Experimental

4.1. General materials and methods

All chemicals and solvents were reagent grade from Aldrich Chemical Co., and solvents were dried by standard techniques. ^{1}H and ^{13}C NMR spectra were measured on a Bruker DRS-300. DSC thermographs were carried out on a Mettler DSC-822 and calibrated with a pure indium sample. All phase transitions are determined by a scan rate of 10.0 °C min^{-1}. Optical polarized microscopy was carried out on Zeiss Axioplan 2 equipped with a hot stage system of Mettler FP90/FP82HT. The UV–vis absorption and fluorescence spectra were obtained using a Jasco V-530 and Hitachi F-4500 spectrometer. All spectra were measured in CH_2Cl_2 at room temperature, and the excitation wavelengths of the fluorescent spectra were 202 nm (for **1a**), 405 nm (for **1b**), and 397 nm (for **2** and **3**). Elemental analyses were performed on a Heraeus CHN-O-Rapid elemental analyzer. The powder diffraction data were collected from the Wiggler-A beam line of the National Synchrotron Radiation Research Center (NSRRC) with a wavelength of 1.3263 Å. The powder samples were charged in Lindemann capillary tubes (80 mm long and 0.01 mm thick) from Charles Supper Co. with an inner diameter of 1.0 mm. The compounds of 1,2-di(alkoxy)benzenes-1,2-bis(3,4-bis(alkoxy)phenyl-1,2-ethanediones), 2,3-bis(3,4-bis(alkoxy)phenyl)quinoxaline-6-carboxylic acids,[12] and ethyl 6-(alkoxy)-2-naphthoates[9a] were prepared by the literature procedures.

4.2. Synthesis of the compounds 1a–c

4.2.1. 1,2-Bis(dodecyloxy)benzene. ^{1}H NMR (300 MHz, $CDCl_3$): δ 0.85 (t, 6H, $-CH_3$, J=6.9 Hz), 1.24–1.45 (m, 36H, $-CH_2$), 1.74–1.84 (m, 4H, $-CH_2$), 3.97 (t, 4H, $-OCH_2$, J=6.6 Hz), 6.86 (s, Ar–H, 4H). ^{13}C NMR (75 MHz, $CDCl_3$): δ 14.14, 22.72, 26.07, 29.38, 29.47, 29.67, 29.73, 31.95, 69.29, 114.12, 121.00, 149.25.

4.2.2. 1,2-Bis(3,4-bis(dodecyloxy)phenyl)-1,2-ethanedione. ^{1}H NMR (300 MHz, $CDCl_3$): δ 0.83–0.88 (m, 12H, $-CH_3$), 1.24–1.45 (m, 72H, $-CH_2$), 1.77–1.86 (m, 8H, $-CH_2$), 4.01–4.05 (m, 8H, $-OCH_2$), 6.81 (d, 2H, Ar–H, J=8.4 Hz), 7.39–7.42 (m, 2H, Ar–H), 7.54 (d, 2H, Ar–H, J=1.8 Hz). ^{13}C NMR (75 MHz, $CDCl_3$): δ 14.14, 22.72, 25.94, 26.00, 28.93, 29.08, 29.40, 29.66, 31.95, 69.11, 69.22, 111.54, 112.19, 126.17, 149.29, 154.97, 193.83.

4.2.3. 2,3-Bis-(3,4-bis(dodecyloxy)phenyl)quinoxaline-6-carboxylic acid ***3***. The solution 1,2-bis(3,4-bis(dodecyloxy)phenyl)-1,2-ethanedione (4.0 g, 0.004 mol) dissolved in 100 mL of THF was stirred with 0.5 mL of glacial acetic acid for 10 min. To the solution, 3,4-diaminobenzoic acid (4.0 g, 0.0051 mol) dissolved in 2.0 mL of DMSO was added and stirred for 24 h under nitrogen atmosphere. The product, isolated as yellow solids was obtained after recrystallization from THF/MeOH. Yield 93%. ^{1}H NMR (300 MHz, $CDCl_3$): δ 0.84–0.88 (m, 12H, $-CH_3$), 1.19–1.41 (m, 72H, $-CH_2$), 1.68–1.83 (m, 8H, $-CH_2$), 3.79–4.01 (m, 8H, $-OCH_2$), 6.81 (d, 2H, Ar–H, J=8.4 Hz), 7.08–7.12 (m, 4H, Ar–H), 8.15 (d, 1H, Ar–H, J=8.7 Hz), 8.32 (d, 1H, Ar–H, J=8.7 Hz), 8.91 (s, 1H, Ar–H). ^{13}C NMR (75 MHz, $CDCl_3$): δ 14.15, 22.72, 26.06, 29.15, 29.22, 29.42, 29.48, 29.73, 31.96, 69.20, 113.04, 115.22, 122.98, 123.15, 129.32, 129.94, 131.08, 131.17, 132.71, 140.12, 143.37, 148.73, 150.19, 150.36, 154.36, 155.16, 170.92.

4.2.4. Ethyl 6-hydroxy-2-naphthoate. To the solution of 6-hydroxy-2-naphthaoic acid (10.0 g, 0.053 mol) dissolved in 100 mL of EtOH was added 2.0 mL of H_2SO_4, and this solution was refluxed for 2 h.

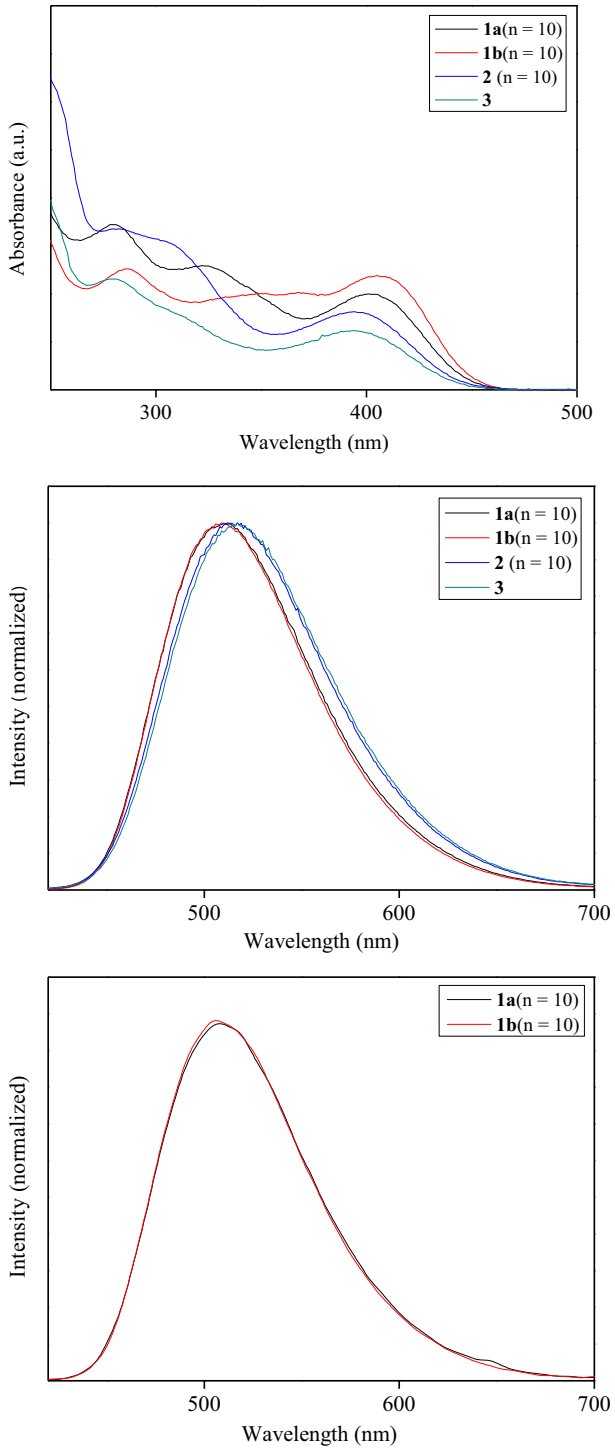

Fig. 6. Absorption (top) and fluorescent spectra (central and bottom) of the compounds **1**–**3**. The excitation wavelengths in PL spectra (central) used were 402 nm (for **1a**-10), 405 nm (**1b**-10), 394 nm (for **2**) and 394 nm (for **3**). The PL spectra of compound **1a**,**b** (bottom) were obtained by using 324 nm (for **1a**-10) and 352 nm (**1b**-10) as excitation wavelengths and the λ_{max}=508 and 505 nm was obtained for **1a** (n=10) and **1b** (n=10).

Table 5
Absorption and emission data[a] of compounds **1**–**3**

Compd	Adsorption λ (nm)	Emission λ_{max} (nm)	Φ_F
1a (n=10)	280, 324, 402	512	0.55
1b (n=10)	287, 352, 405	509	0.57
2 (n=10)	306, 394	517	0.44
3 (n=10)	279, 394	517	0.42

[a] Measured in CH_2Cl_2 solution (1.0×10^{-5} M) at rt. The standard is anthracene (Φ_{fs}=0.27 in hexane solution) and n is reflective index of solvents; $n_{CH_2Cl_2}$ = 1.42440, n_{hexane}=1.37506.

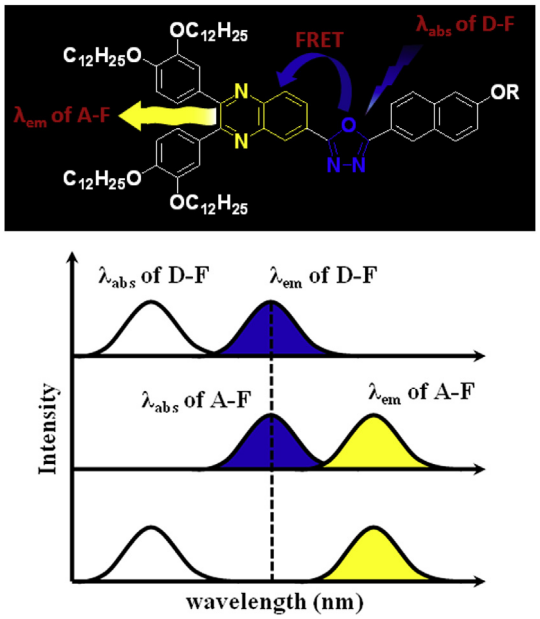

Fig. 7. Schematic diagram of the FRET operated in this system in which 1,3,4-oxadiazole is the donor fluorophore (D–F) and quinoxaline is the acceptor fluorophore (A–F). In the FRET process, blue light originally emitted from 1,3,4-oxadiazole was absorbed by quinoxaline, then emitting yellow light.

The solution was cooled and neutralized with 0.5 M of aqueous NaOH. The solids were collected. The product isolated as white solids were obtained after recrystallization from ethanol. Yield 85%. ^{1}H NMR (300 MHz, $CDCl_3$): δ 3.95 (s, 3H, $-OCH_3$), 5.74 (s, 1H, Ar–OH), 7.15 (d, 2H, Ar–H, J=7.6 Hz), 7.67 (d, 1H, Ar–H, J=8.6 Hz), 7.83 (d, 1H, Ar–H, J=9.7 Hz), 7.98 (d, 1H, Ar–H, J=8.7 Hz), 8.51 (s, 1H, Ar–H). ^{13}C NMR (75 MHz, $CDCl_3$): δ 50.00, 109.31, 118.52, 125.31, 125.91, 126.53, 127.94, 130.72, 131.24, 136.43, 155.65, 167.00.

4.2.5. Ethyl 6-(decyloxy)-2-naphthoate (n=10). The solution of ethyl 6-hydroxy-2-naphthoate (10.0 g, 0.06 mol) dissolved in 150 mL of acetone were added K_2CO_3 (4.5 g, 0.03 mol), KI (5.0 g, 0.03 mol), and 1-bromodecane (16.1 g, 0.06 mol). The solution was refluxed for 48 h under nitrogen atmosphere. The solution was filtered while hot. The filtrate was concentrated to give light brown solids. The products isolated as white solids were obtained after recrystallization from CH_2Cl_2/MeOH. Yield 85%. ^{1}H NMR (300 MHz, $CDCl_3$): δ 0.84–0.87 (t, 3H, $-CH_3$), 1.27–1.48 (m, 14H, $-CH_2$), 1.42 (t, 3H, $-CH_3$, J=7.2 Hz), 1.78–1.88 (m, 2H, $-CH_2$), 4.05 (t, 2H, $-OCH_2$, J=6.6 Hz), 4.37–4.45 (m, 2H, $-OCH_2$), 7.11–7.24 (m, 2H, Ar–H), 7.71 (d, 1H, Ar–H, J=8.7 Hz), 7.81 (d, 1H, Ar–H, J=9 Hz), 8.01 (d, 1H, Ar–H, J=8.4 Hz), 8.51 (s, 1H, Ar–H). ^{13}C NMR (75 MHz, $CDCl_3$): δ 14.07, 14.38, 22.65, 26.05, 29.13, 29.29, 29.37, 29.54, 31.87, 60.82, 68.09, 106.30, 119.81, 125.35, 125.83, 126.66, 127.75, 130.67, 130.73, 137.13, 158.99, 166.88.

4.2.6. 6-(Decyloxy)-2-naphthahydrazide (n=10). The solution of ethyl 6-(decyloxy)-2-naphthoate (5.0 g, 0.02 mol) dissolved in 100 mL of MeOH was added hydrazine monohydrate (7.8 g, 0.2 mol). The solution was refluxed for 12 h. The solution was concentrated to give off-white solids. The products isolated as white solids were obtained after recrystallization from hexane/

MeOH. Yield 90%. ^{1}H NMR (300 MHz, $CDCl_3$): δ 0.91 (t, 3H, $-CH_3$, J=6.9 Hz), 1.32–1.50 (m, 14H, $-CH_2$), 1.77–1.86 (m, 2H, $-CH_2$), 1.96 (s, 2H, $-NH_2$), 4.03 (t, 2H, $-OCH_2$, J=6.6 Hz), 7.08–7.16 (m, 2H, Ar–H), 7.57(m, 1H, –NH), 7.67–7.76 (m, 3H, Ar–H), 8.17 (s, 1H, Ar–H). ^{13}C NMR (75 MHz, $CDCl_3$): δ 14.19, 16.83, 22.75, 25.72, 25.90, 29.27, 31.73, 68.28, 120.22, 124.20, 127.32, 127.68, 127.95, 128.42, 130.54, 136.62, 158.87.

*4.2.7. 2,3-Bis(3,4-bis(dodecyloxy)phenyl)-N′-(6-(alkoxy)-2-naphthoyl)quinoxaline-6-carbohydrazide (**2**, n=10).* The solution of 2,3-bis-(3,4-bis(dodecyloxy)phenyl)quinoxaline-6-carboxylic acid (1.0 g, 0.94 mmol) mixed with 0.3 mL of thionyl chloride (4.0 mmol) was gently refluxed for 4 h under nitrogen atmosphere. The excess of thionyl chloride was removed under reduced vacuum. The compound prepared was then used directly for the following step. The solution of 6-(decyloxy)-2-naphthalhydrazide (0.322 g, 0.94 mmol) dissolved in 30 mL of THF was added dropwise 0.14 mL of triethylamine (1.0 mmol) at ice bath. The solution was stirred at rt for 24 h. The solution was extracted twice with 100 mL of CH_2Cl_2/H_2O. The organic layers were combined and concentrated to give brown solids. The products isolated as yellow-green solids were obtained after recrystallization from ethyl acetate. Yield 75%. ^{1}H NMR (300 MHz, $CDCl_3$): δ 0.84–0.87 (m, 15H, $-CH_3$), 1.26–1.44 (m, 86H, $-CH_2$), 1.62–1.83 (m, 10H, $-CH_2$), 3.73–4.03 (m, 10H, $-OCH_2$), 6.72–6.81 (m, 2H, Ar–H), 6.99–7.10 (m, 6H, Ar–H), 7.55–7.62 (m, 2H, Ar–H), 7.82 (d, 1H, Ar–H, J=8.4 Hz), 8.04 (d, 1H, Ar–H, J=8.7 Hz), 8.15 (d, 1H, Ar–H, J=8.7 Hz), 8.26 (s, 1H, Ar–H), 8.66 (s, 1H, Ar–H), 10.07 (br s, 1H, –NH), 10.33 (br s, 1H, –NH). ^{13}C NMR (75 MHz, $CDCl_3$): δ 14.07, 22.67, 26.05, 29.19, 29.27, 29.37, 29.46, 29.60, 29.68, 31.92, 68.15, 69.20, 106.33, 113.05, 113.12, 115.36, 120.00, 122.97, 123.06, 123.87, 125.94, 127.10, 127.60, 127.71, 128.31, 128.71, 129.49, 130.53, 131.08, 131.22, 132.08, 136.74, 139.96, 142.41, 148.66, 148.76, 150.19, 150.33, 154.06, 154.59, 158.91, 164.09, 165.12. MS (HRFAB): calcd for M^+: 1387.0566. Found: 1387.0566. Anal. Calcd for $C_{90}H_{138}N_4O_7$: C, 77.87; H, 10.02. Found C, 77.21; H, 9.83.

*4.2.8. 2,3-Bis(3,4-bis(dodecyloxy)phenyl)-N′-(6-(octyloxy)-2-naphthoyl)quinoxaline-6-carbohydrazide (**2**, n=8).* ^{1}H NMR (300 MHz, $CDCl_3$): δ 0.84–0.88 (m, 15H, $-CH_3$), 1.26–1.44 (m, 82H, $-CH_2$), 1.64–1.83 (m, 10H, $-CH_2$), 3.72–4.02 (m, 10H, $-OCH_2$), 6.72–6.81 (m, 2H, Ar–H), 6.99–7.10 (m, 6H, Ar–H), 7.54–7.60 (m, 2H, Ar–H), 7.81 (d, 1H, Ar–H, J=8.7 Hz), 8.03 (d, 1H, Ar–H, J=8.7 Hz), 8.15 (d, 1H, Ar–H, J=8.7 Hz), 8.24 (s, 1H, Ar–H), 8.65 (s, 1H, Ar–H), 10.15 (br s, 1H, –NH), 10.40 (br s, 1H, –NH). ^{13}C NMR (75 MHz, $CDCl_3$): δ 14.08, 22.66, 26.03, 29.16, 29.24, 29.37, 29.46, 29.68, 31.91, 68.10, 69.13, 106.23, 112.88, 112.97, 115.20, 119.97, 122.88, 122.98, 123.84, 125.86, 127.06, 127.52, 127.66, 128.31, 128.76, 129.50, 130.51, 131.09, 131.24, 131.98, 136.69, 140.00, 142.46, 148.56, 148.66, 150.05, 150.19, 154.08, 154.61, 158.85, 164.16, 165.16. MS (HRFAB): calcd for M^+: 1359.0253. Found: 1359.0265. Anal. Calcd for $C_{88}H_{134}N_4O_7$: C, 77.71; H, 9.93. Found C, 77.81; H, 9.33.

*4.2.9. 2,3-Bis(3,4-bis(dodecyloxy)phenyl)-N′-(6-(dodecyloxy)-2-naphthoyl)quinoxaline-6-carbohydrazide (**2**, n=12).* ^{1}H NMR (300 MHz, $CDCl_3$): δ 0.84–0.86 (m, 15H, $-CH_3$), 1.25–1.44 (m, 90H, $-CH_2$), 1.66–1.80 (m, 10H, $-CH_2$), 3.73–4.02 (m, 10H, $-OCH_2$), 6.71–6.80 (m, 2H, Ar–H), 6.98–7.10 (m, 6H, Ar–H), 7.54–7.61 (m, 2H, Ar–H), 7.81 (d, 1H, Ar–H, J=8.4 Hz), 8.03 (d, 1H, Ar–H, J=8.7 Hz), 8.15 (d, 1H, Ar–H, J=9.0 Hz), 8.25 (s, 1H, Ar–H), 8.65 (s, 1H, Ar–H), 10.15 (br s, 1H, –NH), 10.41 (br s, 1H, –NH). ^{13}C NMR (75 MHz, $CDCl_3$): δ 14.10, 22.68, 26.05, 29.17, 29.24, 29.38, 29.47, 29.69, 31.92, 68.12, 69.14, 106.26, 112.99, 115.22, 120.02, 122.99, 123.85, 125.89, 127.09, 127.53, 127.68, 128.31, 128.76, 129.52, 130.53, 131.11, 131.24, 132.01, 136.72, 140.02, 142.47, 148.58, 148.68, 150.07, 150.21, 154.11, 154.63, 158.88, 164.10, 165.24. MS (HRFAB): calcd for M^+: 1415.0879. Found: 1415.0874. Anal. Calcd for $C_{92}H_{142}N_4O_7$: C, 78.03; H, 10.11. Found C, 77.14; H, 10.28.

*4.2.10. 2, 3-Bis(3,4-bis(dodecyloxy)phenyl)-N′-(6-(tetradecyloxy)-2-naphthoyl)quinoxaline-6-carbohydrazide (**2**, n=14).* ^{1}H NMR (300 MHz, $CDCl_3$): δ 0.84–0.88 (m, 15H, $-CH_3$), 1.24–1.44 (m, 94H, $-CH_2$), 1.66–1.83 (m, 10H, $-CH_2$), 3.73–3.99 (m, 10H, $-OCH_2$), 6.69–6.80 (m, 2H, Ar–H), 6.97–7.05 (m, 6H, Ar–H), 7.50–7.57 (m, 2H, Ar–H), 7.80 (d, 1H, Ar–H, J=8.4 Hz), 8.00 (d, 1H, Ar–H, J=8.7 Hz), 8.14 (d, 1H, Ar–H, J=8.7 Hz), 8.23 (s, 1H, Ar–H), 8.65 (s, 1H, Ar–H), 10.22 (br s, 1H, –NH), 10.48 (br s, 1H, –NH). ^{13}C NMR (75 MHz, $CDCl_3$): δ 14.08, 22.67, 26.04, 29.16, 29.24, 29.37, 29.47, 29.68, 31.92, 68.09, 69.12, 106.21, 112.86, 112.96, 115.20, 119.92, 122.89, 122.98, 123.85, 125.87, 127.02, 128.33, 128.79, 129.46, 130.51, 131.08, 131.25, 131.99, 136.66, 139.97, 142.44, 148.53, 148.66, 150.03, 150.18, 154.05, 154.58, 164.32, 165.36. MS (HRFAB): calcd for M^+: 1443.1192. Found: 1443.1201. Anal. Calcd for $C_{94}H_{146}N_4O_7$: C, 78.18; H, 10.19. Found C, 78.90; H, 10.35.

*4.2.11. 2,3-Bis(3,4-bis(dodecyloxy)phenyl)-N′-(6-(hexadecyloxy)-2-naphthoyl)quinoxaline-6-carbohydrazide (**2**, n=16).* ^{1}H NMR (300 MHz, $CDCl_3$): δ 0.84–0.88 (m, 15H, $-CH_3$), 1.24–1.44 (m, 98H, $-CH_2$), 1.64–1.81 (m, 10H, $-CH_2$), 3.74–4.03 (m, 10H, $-OCH_2$), 6.73–6.81 (m, 2H, Ar–H), 7.00–7.10 (m, 6H, Ar–H), 7.58–7.64 (m, 2H, Ar–H), 7.82 (d, 1H, Ar–H, J=8.4 Hz), 8.10 (d, 1H, Ar–H, J=8.7 Hz), 8.15 (d, 1H, Ar–H, J=8.7 Hz), 8.26 (s, 1H, Ar–H), 8.65 (s, 1H, Ar–H), 9.99 (br s, 1H, –NH), 10.26 (br s, 1H, –NH). ^{13}C NMR (75 MHz, $CDCl_3$): δ 14.10, 22.69, 26.05, 29.17, 29.24, 29.38, 29.47, 29.68, 31.93, 68.14, 69.14, 106.28, 112.99, 115.20, 120.08, 122.90, 123.00, 123.82, 125.86, 127.16, 127.51, 127.70, 128.27, 128.71, 129.60, 130.54, 131.11, 131.23, 131.97, 136.76, 140.04, 142.51, 148.61, 148.69, 150.09, 150.22, 154.15, 154.68, 158.92, 163.88, 164.88. MS (HRFAB): calcd for M^+: 1471.1505. Found: 1471.1505. Anal. Calcd for $C_{96}H_{150}N_4O_7$: C, 78.32; H, 10.27. Found C, 77.94; H, 10.17.

*4.2.12. 2-(2,3-Bis(3,4-bis(dodecyloxy)phenyl)quinoxalin-6-yl)-5-(6-(decyloxy)naphthalen-2-yl)-1,3,4-oxadiazole (**1a**, n=10).* The solution of 2,3-bis(3,4-bis(dodecyloxy)phenyl)-*N*′-(6-(decyloxy)-2-naphthoyl)-quinoxaline-6-carbohydrazide (1.0 g, 0.36 mmol) dissolved in 10 mL of phosphoryl chloride was refluxed for 24 h. The solution slowly turned reddish-black in color. The solution was cooled at room temperature, and then the solution was slowly poured into 300 mL of icy water. After stirring for 2 h, the orange-red solids were filtered and collected. The solids were dissolved in 25 mL of dichloromethane and extracted with 150 mL of 1.0 M $NaOH_{(aq)}$ for 2 h. The yellow-brown solids were collected. The products isolated as bright yellow solids were obtained after recrystallization from THF/methanol or by silica gel chromatography eluting with hexane/ethyl acetate. Yield 55%. ^{1}H NMR (300 MHz, $CDCl_3$): δ 0.84–0.87 (m, 15H, $-CH_3$), 1.25–1.45 (m, 86H, $-CH_2$), 1.69–1.90 (m, 10H, $-CH_2$), 3.80–4.12 (m, 10H, $-OCH_2$), 6.82–6.87 (m, 2H, Ar–H), 7.10–7.23 (m, 6H, Ar–H), 7.83–7.88 (m, 2H, Ar–H), 8.18 (d, 1H, Ar–H, J=8.7 Hz), 8.26 (d, 1H, Ar–H, J=8.7 Hz), 8.52 (d, 1H, Ar–H, J=8.7 Hz), 8.57 (s, 1H, Ar–H), 8.89 (s, 1H, Ar–H). ^{13}C NMR (75 MHz, $CDCl_3$): δ 14.07, 22.67, 26.05, 29.18, 29.25, 29.37, 29.45, 29.57, 29.68, 31.92, 68.27, 69.28, 106.76, 113.23, 115.45, 118.62, 120.43, 122.96, 123.11, 123.80, 124.75, 127.19, 127.39, 127.64, 127.78, 128.23, 130.09, 130.39, 131.17, 136.52, 140.58, 142.24, 148.85, 150.34, 150.44, 154.50, 159.04, 163.84, 165.52. MS (HRESI): calcd for M^+: 1370.0773. Found: 1370.0542. Anal. Calcd for $C_{90}H_{136}N_4O_6$: C, 78.78; H, 10.14. Found C, 78.76; H, 10.10.

*4.2.13. 2-(2,3-Bis(3,4-bis(dodecyloxy)phenyl)quinoxalin-6-yl)-5-(6-(octyloxy)naphthalen-2-yl)-1,3,4-oxadiazole (**1a**, n=8).* ^{1}H NMR (300 MHz, $CDCl_3$): δ 0.83–0.88 (m, 15H, $-CH_3$), 1.25–1.47 (m, 82H, $-CH_2$), 1.67–1.90 (m, 10H, $-CH_2$), 3.80–4.12 (m, 10H, $-OCH_2$),

6.82–6.87 (m, 2H, Ar–H), 7.09–7.22 (m, 6H, Ar–H), 7.83–7.89 (m, 2H, Ar–H), 8.18 (d, 1H, Ar–H, *J*=8.7 Hz), 8.25 (d, 1H, Ar–H, *J*=8.7 Hz), 8.52 (d, 1H, Ar–H, *J*=8.7 Hz), 8.57 (s, 1H, Ar–H), 8.88 (s, 1H, Ar–H). ^{13}C NMR (75 MHz, $CDCl_3$): δ 14.09, 22.69, 26.05, 29.18, 29.25, 29.38, 29.46, 29.70, 31.83, 31.93, 68.27, 69.25, 106.74, 113.21, 115.38, 118.64, 120.44, 122.90, 123.04, 123.81, 124.69, 127.13, 127.39, 127.79, 128.23, 130.18, 130.40, 131.29, 131.39, 136.52, 140.68, 142.39, 148.82, 150.25, 150.35, 154.47, 154.58, 159.04, 163.89, 165.51. MS (HRESI): calcd for M^+: 1342.0147. Found: 1342.0214. Anal. Calcd for $C_{88}H_{132}N_4O_6$: C, 78.76; H, 9.91. Found C, 78.90; H, 10.09.

*4.2.14. 2-(2,3-Bis(3,4-bis(dodecyloxy)phenyl)quinoxalin-6-yl)-5-(6-(dodecyloxy)naphthalen-2-yl)-1,3,4-oxadiazole (**1a**, n=12).* ^{1}H NMR (300 MHz, $CDCl_3$): δ 0.84–0.87 (m, 15H, $-CH_3$), 1.25–1.45 (m, 90H, $-CH_2$), 1.69–1.82 (m, 10H, $-CH_2$), 3.80–4.12 (m, 10H, $-OCH_2$), 6.82–6.87 (m, 2H, Ar–H), 7.10–7.23 (m, 6H, Ar–H), 7.83–7.89 (m, 2H, Ar–H), 8.18 (d, 1H, Ar–H, *J*=8.7 Hz), 8.27 (d, 1H, Ar–H, *J*=8.7 Hz), 8.53 (d, 1H, Ar–H, *J*=8.7 Hz), 8.57 (s, 1H, Ar–H), 8.90 (s, 1H, Ar–H). ^{13}C NMR (75 MHz, $CDCl_3$): δ 14.08, 22.68, 26.05, 29.19, 29.25, 29.38, 29.46, 29.69, 31.93, 68.27, 69.28, 106.75, 113.23, 115.44, 118.61, 120.42, 122.95, 123.11, 123.79, 124.75, 127.19, 127.39, 127.63, 127.78, 128.23, 130.08, 130.39, 131.22, 136.51, 140.58, 142.21, 148.84, 150.34, 150.44, 154.42, 154.49, 163.84, 165.51. MS (HRESI): calcd for M^+: 1398.0773. Found: 1398.0854. Anal. Calcd for $C_{92}H_{140}N_4O_6$: C, 79.03; H, 10.09. Found C, 79.18; H, 10.10.

*4.2.15. 2-(2,3-Bis(3,4-bis(dodecyloxy)phenyl)quinoxalin-6-yl)-5-(6-(tetradecyloxy) naphthalen-2-yl)-1,3,4-oxadiazole (**1a**, n=14).* ^{1}H NMR (300 MHz, $CDCl_3$): δ 0.84–0.88 (m, 15H, $-CH_3$), 1.25–1.45 (m, 94H, $-CH_2$), 1.72–1.88 (m, 10H, $-CH_2$), 3.82–4.12 (m, 10H, $-OCH_2$), 6.82–6.87 (m, 2H, Ar–H), 7.11–7.23 (m, 6H, Ar–H), 7.83–7.89 (m, 2H, Ar–H), 8.18 (d, 1H, Ar–H, *J*=8.7 Hz), 8.31 (d, 1H, Ar–H, *J*=8.4 Hz), 8.54 (d, 1H, Ar–H, *J*=8.1 Hz), 8.58 (s, 1H, Ar–H), 8.92 (s, 1H, Ar–H). ^{13}C NMR (75 MHz, $CDCl_3$): δ 14.09, 22.68, 26.05, 29.18, 29.23, 29.38, 29.45, 29.68, 31.93, 68.27, 69.28, 106.75, 113.18, 115.40, 118.57, 120.45, 123.03, 123.19, 123.81, 124.88, 127.36, 127.44, 127.80, 128.23, 129.95, 130.42, 130.77, 130.94, 136.54, 140.43, 141.99, 148.85, 150.42, 154.41, 159.05, 163.80, 165.57. MS (HRESI): calcd for M^+: 1426.1086. Found: 1426.1179. Anal. Calcd for $C_{94}H_{144}N_4O_6$: C, 79.16; H, 10.18. Found C, 79.11; H, 10.39.

*4.2.16. 2-(2,3-Bis(3,4-bis(dodecyloxy)phenyl)quinoxalin-6-yl)-5-(6-(hexadecyloxy) naphthalen-2-yl)-1,3,4-oxadiazole (**1a**, n=16).* ^{1}H NMR (300 MHz, $CDCl_3$): δ 0.83–0.88 (m, 15H, $-CH_3$), 1.18–1.43 (m, 98H, $-CH_2$), 1.65–1.90 (m, 10H, $-CH_2$), 3.82–4.12 (m, 10H, $-OCH_2$), 6.82–6.86 (m, 2H, Ar–H), 7.10–7.22 (m, 6H, Ar–H), 7.83–7.89 (m, 2H, Ar–H), 8.18 (d, 1H, Ar–H, *J*=8.4 Hz), 8.28 (d, 1H, Ar–H, *J*=8.1 Hz), 8.53 (d, 1H, Ar–H, *J*=7.8 Hz), 8.58 (s, 1H, Ar–H), 8.91 (s, 1H, Ar–H). ^{13}C NMR (75 MHz, $CDCl_3$): δ 14.08, 22.67, 26.04, 29.17, 29.23, 29.37, 29.45, 29.68, 31.92, 68.25, 69.27, 106.72, 113.18, 115.40, 118.57, 120.43, 122.99, 123.15, 123.79, 124.79, 127.26, 127.40, 127.57, 127.78, 128.21, 130.03, 130.40, 131.10, 136.51, 140.50, 142.11, 148.82, 150.35, 154.45, 159.03, 163.81, 165.52. MS (HRESI): calcd for M^+: 1454.14. Found: 1454.15. Anal. Calcd for $C_{96}H_{148}N_4O_6$: C, 79.18; H, 10.38. Found C, 79.26; H, 10.36.

*4.2.17. 2-(2,3-Bis(3,4-bis(dodecyloxy)phenyl)quinoxalin-6-yl)-5-(6-(alkoxy)naphthalen-2-yl)-1,3,4-thiadiazole (**1b**, n=10).* The solution of 2,3-bis(3,4-bis(dodecyloxy)phenyl)-*N*′-(6-(decyloxy)-2-naphthoyl)-quinoxaline-6-carbohydrazide (1.0 g, 0.36 mmol) dissolved in 10 mL of dry pyridine. The solution was gently heated until all solids were dissolved. To the solution was then added phosphorus pentasulfide (1.12 g, 5.0 mol), and then refluxed for 24 h. The solution was extracted twice with 100 mL of CH_2Cl_2/H_2O. The organic layers were combined and concentrated to give brown solids. The products isolated as yellow-green solids were obtained after recrystallization from THF/methanol or by silica gel chromatography eluting with hexane/ethyl acetate. Yield 45%. ^{1}H NMR (300 MHz, $CDCl_3$): δ 0.84–0.89 (m, 15H, $-CH_3$), 1.25–1.43 (m, 86H, $-CH_2$), 1.67–1.89 (m, 10H, $-CH_2$), 3.80–4.10 (m, 10H, $-OCH_2$), 6.81–6.86 (m, 2H, Ar–H), 7.09–7.22 (m, 6H, Ar–H), 7.78–7.85 (m, 2H, Ar–H), 8.10 (d, 1H, Ar–H, *J*=8.4 Hz), 8.23 (d, 1H, Ar–H, *J*=8.7 Hz), 8.39 (s, 1H, Ar–H), 8.52 (d, 1H, Ar–H, *J*=8.4 Hz), 8.64 (s, 1H, Ar–H). ^{13}C NMR (75 MHz, $CDCl_3$): δ 14.08, 22.67, 26.04, 29.17, 29.23, 29.37, 29.45, 29.57, 29.69, 31.92, 68.22, 69.25, 106.66, 113.20, 115.39, 120.32, 122.94, 123.09, 125.06, 127.74, 128.00, 128.20, 128.42, 128.73, 129.87, 130.24, 131.12, 131.26, 136.26, 140.57, 141.99, 148.82, 150.30, 150.35, 154.16, 158.77, 166.64, 169.30. MS (HRESI): calcd for M^+: 1386.0231. Found: 1386.0323. Anal. Calcd for $C_{90}H_{136}N_4O_5S$: C, 77.87; H, 10.02. Found C, 77.81; H, 10.02.

*4.2.18. 2-(2,3-Bis(3,4-bis(dodecyloxy)phenyl)quinoxalin-6-yl)-5-(6-(dodecyloxy)naphthalen-2-yl)-1,3,4-thiadiazole (**1b**, n=12).* ^{1}H NMR (300 MHz, $CDCl_3$): δ 0.84–0.89 (m, 15H, $-CH_3$), 1.25–1.45 (m, 90H, $-CH_2$), 1.61–1.87 (m, 10H, $-CH_2$), 3.80–4.11 (m, 10H, $-OCH_2$), 6.81–6.86 (m, 2H, Ar–H), 7.09–7.23 (m, 6H, Ar–H), 7.79–7.86 (m, 2H, Ar–H), 8.10 (d, 1H, Ar–H, *J*=8.7 Hz), 8.21 (d, 1H, Ar–H, *J*=8.7 Hz), 8.39 (s, 1H, Ar–H), 8.52 (d, 1H, Ar–H, *J*=8.7 Hz), 8.62 (s, 1H, Ar–H). ^{13}C NMR (75 MHz, $CDCl_3$): δ 14.08, 22.68, 26.04, 29.17, 29.23, 29.37, 29.45, 29.68, 31.92, 68.22, 69.23, 106.67, 113.22, 115.31, 115.38, 120.33, 122.86, 123.01, 125.07, 127.75, 127.89, 128.19, 128.43, 128.93, 129.98, 130.24, 131.15, 131.33, 131.42, 136.26, 140.80, 142.15, 148.81, 150.19, 150.26, 154.22, 154.28, 158.77, 166.73, 169.27. MS (HRESI): calcd for M^+: 1414.0544. Found: 1414.0617. Anal. Calcd for $C_{92}H_{140}N_4O_5S$: C, 78.14; H, 9.98. Found C, 78.39; H, 9.99.

*4.2.19. 2-(2,3-Bis(3,4-bis(dodecyloxy)phenyl)quinoxalin-6-yl)-5-(6-(hexadecyloxy)naphthalen-2-yl)-1,3,4-thiadiazole (**1b**, n=16).* ^{1}H NMR (300 MHz, $CDCl_3$): δ 0.84–0.88 (m, 15H, $-CH_3$), 1.19–1.31 (m, 98H, $-CH_2$), 1.54–1.90 (m, 10H, $-CH_2$), 3.80–4.12 (m, 10H, $-OCH_2$), 6.81–6.86 (m, 2H, Ar–H), 7.09–7.23 (m, 6H, Ar–H), 7.80–7.86 (m, 2H, Ar–H), 8.12 (d, 1H, Ar–H, *J*=8.4 Hz), 8.22 (d, 1H, Ar–H, *J*=8.7 Hz), 8.40 (s, 1H, Ar–H), 8.53 (d, 1H, Ar–H, *J*=8.7 Hz), 8.63 (s, 1H, Ar–H). ^{13}C NMR (75 MHz, $CDCl_3$): δ 14.08, 22.68, 26.03, 29.17, 29.23, 29.37, 29.45, 29.68, 31.92, 68.23, 69.23, 106.67, 113.22, 115.37, 120.33, 122.85, 123.01, 125.07, 127.75, 127.89, 128.19, 128.43, 128.93, 129.98, 130.24, 131.15, 131.33, 131.42, 136.26, 140.80, 142.16, 148.80, 150.18, 150.25, 154.22, 154.28, 158.77, 166.73, 169.27. MS (HRESI): calcd for M^+: 1470.1170. Found: 1470.1237. Anal. Calcd for $C_{96}H_{148}N_4O_5S$: C, 78.42; H, 10.15. Found C, 78.42; H, 9.72.

Acknowledgements

We thank the National Science Council of Taiwan, ROC (NSC-100-2113-M-008-00-MY2) for generous support of this work.

References and notes

1. (a) Leung, M. K.; Yang, W. H.; Chung, C. N.; Lee, J. H.; Lin, C. F.; Wei, M. K.; Liu, Y. H. *Org. Lett.* **2012**, *14*, 4986–4989; (b) Zheng, Y.; Batanov, A. S.; Jankus, V.; Dias, F. B.; Bryce, M. R.; Monkman, A. P. *J. Org. Chem.* **2011**, *76*, 8300–8310; (c) Reddya, M. A.; Malleshama, G.; Thomas, A.; Srinivasa, K.; Rao, V. J.; Bhanuprakash, K.; Giribabu, L. .; Grover, R.; Kumar, A.; Kamalasanan, M. N.; Srivastava, R. *Synth. Met.* **2011**, *161*, 869–880; (d) Reddy, M. A.; Thomas, A.; Srinivas, K.; Rao, V. J.; Bhanuprakash, K.; Sridhar, B.; Kumar, A.; Kamalasanan, M. N.; Srivastava, R. *J. Mater. Chem.* **2009**, *19*, 6172–6184.
2. Dimitrowa, K.; Hauschild, J.; Zaschke, H.; Schubert, H. *J. Prakt. Chem.* **1980**, *322*, 933–944.
3. (a) Wang, L.; He, W.; Wang, M.; Wei, M.; Sun, J.; Chen, X.; Yang, H. *Liq. Cryst.* **2013**, *40*, 354–367; (b) Han, J.; Wang, Q.; Chang, X. Y.; Zhu, L. R. *Liq. Cryst.* **2012**, *39*, 669–674; (c) Wang, L.; Yu, L.; Xiao, X.; Wang, Z.; Yang, P.; He, W.; Yang, H. *Liq. Cryst.* **2012**, *39*, 629–638; (d) Wang, H.; Zheng, Z.; Shen, D. *Liq. Cryst.* **2012**, *39*, 99–103; (e) Majumdar, K. C.; Shyam, P. K.; Shankar Rao, D. S.; Prasad, S. K. *Liq. Cryst.* **2012**, *39*, 1117–1123; (f) Han, J.; Zhang, M.; Wang, F.; Geng, Q. *Liq. Cryst.* **2010**, *37*, 1471–1478; (g) Prajapati, A. K.; Modi, V. *Phase Transitions* **2010**, *83*, 634–649; (h) Tomma, J. H.; Rouil, I. H.; Al; Dujaili, A. H. *Mol. Cryst. Liq. Cryst.*

2009, *501*, 3–19; (i) Parra, M. L.; Elgueta, E. Y.; Jimenez, V.; Hidalgo, P. I. *Liq. Cryst.* **2009**, *36*, 301–317; (j) Han, J.; Zhang, F. Y.; Wang, J. Y.; Wang, Y. M.; Pang, M. L.; Meng, J. B. *Liq. Cryst.* **2009**, *36*, 825–833; (k) Han, J.; Chang, X. Y.; Wang, Y. M.; Pang, M. L.; Meng, J. B. *J. Mol. Struct.* **2009**, *937*, 122–130; (l) Han, J.; Zhang, F. Y.; Chen, Z.; Wang, J. Y.; Zhu, L. R.; Pang, M. L.; Meng, J. B. *Liq. Cryst.* **2008**, *35*, 1359–1365; (m) Han, J.; Chang, X. Y.; Zhu, L. R.; Wang, Y. M.; Meng, J. B.; Lai, S. W.; Chui, S. S. Y. *Liq. Cryst.* **2008**, *35*, 1379–1394; (n) Celso, F. L.; Pibiri, I.; Triolo, A.; Triolo, R.; Pace, A.; Buscemi, S.; Vivona, N. *J. Mater. Chem.* **2007**, *17*, 1201–1208; (o) He, C. F.; Richards, G. J.; Kelly, S. M.; Contoret, A. E. A.; O'Neill, M. *Liq. Cryst.* **2007**, *34*, 1249–1267; (p) Liao, C. T.; Wang, Y. J.; Huang, C. S.; Sheu, H. S.; Lee, G. H.; Lai, C. K. *Tetrahedron* **2007**, *63*, 12437–12445.

4. (a) Frizon, T. E.; Rampon, D. S.; Gallardo, H.; Merlo, A. A.; Schneider, P. H.; Rodrigues, O. E. D.; Braga, A. L. *Liq. Cryst.* **2012**, *39*, 769–777; (b) Qu, S.; Wang, L.; Liu, X.; Li, M. *Chem.—Eur. J.* **2011**, *17*, 3512–3518; (c) Zhang, P.; Bai, B.; Wang, H.; Qu, S.; Yu, Z.; Ran, X.; Li, M. *Liq. Cryst.* **2009**, *36*, 7–12; (d) Srivastava, R. M.; Ricardo, A. W.; Filho, N.; Schneider, R.; Vieira, A.; Gallardo, H. *Liq. Cryst.* **2008**, *35*, 737–742; (e) Wang, H.; Zhang, F.; Bai, B.; Zhang, P.; Shi, J.; Yu, D.; Zhao, Y.; Wang, Y.; Li, M. *Liq. Cryst.* **2008**, *35*, 905–912; (f) Zhang, P.; Qu, S.; Wang, H.; Bai, B.; Li, M. *Liq. Cryst.* **2008**, *35*, 389–394; (g) Chai, C.; Yang, Q.; Fan, X.; Chen, X.; Shen, Z.; Zhou, Q. *Liq. Cryst.* **2008**, *35*, 133–141; (h) Qu, S.; Li, M. *Tetrahedron* **2007**, *63*, 12429–12436.
5. (a) Barbera, J.; Godoy, M. A.; Hidalgo, P. I.; Parra, M. L.; Ulloa, J. A.; Vergara, J. M. *Liq. Cryst.* **2011**, *38*, 679–688; (b) Yelamaggad, C. V.; Achalkumar, A. S.; Shankar Rao, D. S.; Prasad, S. K. *J. Org. Chem.* **2009**, *74*, 3168–3171.
6. (a) Tang, J.; Huang, R.; Gao, H.; Cheng, X.; Prehm, M.; Tschierske, C. *RSC Adv.* **2012**, *2*, 2842–2847; (b) Vieira, A. A.; Gallardo, H.; Barbera, J.; Romero, P.; Serrano, J. L.; Sierra, T. *J. Mater. Chem.* **2011**, *21*, 5916–5922; (c) Gallardo, H.; Ferreira, M.; Vieira, A. A.; Westphal, E.; Molin, F.; Eccher, J.; Bechtold, I. H. *Tetrahedron* **2011**, *67*, 9491–9499; (d) Choi, E. J.; Xu, F. *Mol. Cryst. Liq. Cryst.* **2010**, *529*, 147–156.
7. (a) Picken, S. J.; Dingemans, T. J.; Madsen, L. A.; Francescangeli, O.; Samulski, E. T. *Liq. Cryst.* **2012**, *39*, 19–23; (b) Prajapati, A. K.; Modi, V. *Liq. Cryst.* **2011**, *38*, 191–199; (c) Bates, M. A. *Chem. Phys. Lett.* **2007**, *437*, 189–192; (d) Acharya, B. R.; Primak, A.; Dingemans, T. J.; Samulski, E. T.; Kumar, S. *Pramana-J. Phys.* **2003**, *61*, 231–237.
8. (a) Han, J.; Geng, Q.; Chen, W. .; Zhu, L.; Wu, Q.; Wang, Q. *Supramol. Chem.* **2012**, *24*, 157–164; (b) Martin, P. J.; Bruce, D. W. *Liq. Cryst.* **2007**, *34*, 767–774.
9. (a) Kuo, H. M.; Li, S. Y.; Sheu, H. S.; Lai, C. K. *Tetrahedron* **2012**, *68*, 7331–7337; (b) Wen, C. R.; Wang, Y. J.; Wang, H. C.; Sheu, H. S.; Lee, G. H.; Lai, C. K. *Chem. Mater.* **2005**, *17*, 1646–1654.
10. (a) Prajapati, A. K.; Modi, V. *Liq. Cryst.* **2010**, *37*, 407–415; (b) Seed, A. *Chem. Soc. Rev.* **2007**, *36*, 2046–2069; (c) Dingemans, T. J.; Samulski, E. T. *Liq. Cryst.* **2000**, *27*, 131–136.
11. (a) Voisin, E.; Foster, E. J.; Rakotomalala, M.; Williams, V. E. *Chem. Mater.* **2009**, *21*, 3251–3261; (b) Foster, E. J.; Jones, R. B.; Lavigueur, C.; Williams, V. E. *J. Am. Chem. Soc.* **2006**, *128*, 8569–8574; (c) Foster, E. J.; Lavigueur, C.; Ke, Y. C.; Williams, V. E. *J. Mater. Chem.* **2005**, *15*, 4062–4068; (d) Bojinov, V. B.; Grabchev, I. K. *Org. Lett.* **2003**, *5*, 2185–2187; (e) Boden, N.; Bushby, R. J.; Liu, Q.; Lozman, O. R. *J. Mater. Chem.* **2001**, *11*, 1612–1617.
12. Chen, C. J.; Wu, Y. C.; Sheu, H. S.; Lee, G. H.; Lai, C. K. *Tetrahedron* **2011**, *67*, 114–124.
13. (a) Ziessel, R.; Pickaert, G.; Camerel, F.; Donnio, B.; Guillon, D.; Cesario, M.; Prangé, T. *J. Am. Chem. Soc.* **2004**, *126*, 12403–12413; (b) Donnio, B.; Heinrich, B.; Allouchi, H.; Kain, J.; Diele, S.; Guillon, D.; Bruce, D. W. *J. Am. Chem. Soc.* **2004**, *126*, 15258–15268; (c) Morale, F.; Date, R. W.; Guillon, D.; Bruce, D. W.; Finn, R. L.; Wilson, C.; Blake, A. J.; Schröder, M.; Donnio, B. *Chem.—Eur. J.* **2003**, *9*, 2484–2501; (d) Attias, A. J.; Cavalli, C.; Donnio, B.; Guillon, D. P.; Hapiot, M. J. *Chem. Mater.* **2002**, *14*, 375–384.
14. (a) Liu, Z.; He, W.; Guo, Z. *Chem. Soc. Rev.* **2013**, *42*, 1568–1600; (b) Yang, C. C.; Hsu, C. J.; Chou, P. T.; Cheng, H. C.; Su, Y. O.; Leung, M. K. *J. Phys. Chem. B* **2010**, *114*, 756–768; (c) Bolton, O.; Kim, J. *J. Mater. Chem.* **2007**, *17*, 1981–1988.